# Hadron physics with hyperon beams

C. Quigg*

*Fermi National Accelerator Laboratory,[†] Batavia, Illinois 60510*

Jonathan L. Rosner[‡]

*School of Physics and Astronomy, University of Minnesota, Minneapolis, Minnesota 55455*
(Received 2 February 1976)

Some quantitative expectations are given for hadronic experiments with hyperon beams. These include measurements of total and elastic cross sections, diffractive production of nonresonant and resonant states, charge- and hypercharge-exchange reactions, studies of "missing" strange resonances, uses of polarized hyperon beams, and searches for new particles. Some comments are added about Coulomb dissociation of hyperons.

## I. INTRODUCTION

A great deal has been learned in strong-interaction physics as a result of the large variety of secondary hadron beams. For the past 15 years these have included charged pions and kaons, neutrons, protons and antiprotons, and (more recently) long-lived neutral kaons, $\Lambda$, $\bar{\Lambda}$, and $\Sigma^-$. Systematic experiments using hyperon beams are now being planned at the CERN Super Proton Synchrotron and at Fermilab. These beams will be very useful in the study of weak interactions of hyperons, for which a number of quantitative predictions exist.[1] The hyperon beams contemplated also will permit a wide range of hadron experiments, however. In the present article, we have listed as many of these experiments as we could. Some have been discussed before[2-5]; others are new. In all cases we have tried to estimate quantitatively the "interesting" levels of precision.

Section II discusses total cross sections of hyperons and antihyperons on nucleons. The standard quark-model predictions are reviewed, and a more general discussion based only on SU(3) is given. Section III is devoted to elastic scattering, with particular emphasis on real parts of forward amplitudes, slopes, and experiments at $|t| \simeq 1$ GeV$^2$. In Sec. IV we discuss the states (both resonant and nonresonant) that can be produced diffractively from hyperons. Section V deals with a few simple observations regarding charge-exchange and hypercharge-exchange reactions. These will be treated in detail in a separate publication.[6]

In Sec. VI we show that certain channels accessible to hyperon beam experiments are expected to contain many more resonances than have been observed up to now. These include $\Lambda\pi$, $\Sigma\pi$ (particularly $I = 1$), and $\Xi\pi$. The "resonance deficit" is estimated in these channels, and suggestions are made for making up the deficit by means of hyper-on-pion scattering experiments.

The $\Lambda$ beams produced at Fermilab appear to be polarized at high $p_\perp$.[7] If this effect can be understood and controlled, the prospect exists for a whole range of experiments using high-energy polarized hyperon beams. Some suggestions are made in Sec. VIII.

Coulomb dissociation of hyperons,[2] though not a hadronic process, is mentioned briefly in Sec. VIII for completeness. In Sec. IX we discuss some additional merits of the negative strangeness of hyperon beams: They might be useful in producing particles with new quantum numbers, and they could add insight regarding inclusive processes, particularly those involving high-transverse-momentum secondaries. Section X contains our conclusions.

## II. TOTAL CROSS SECTIONS OF HYPERONS AND ANTIHYPERONS ON NUCLEONS

Let us begin by discussing baryon-baryon systems. A "first guess" at hyperon-nucleon total cross sections follows from the additive quark model. The total cross section of a strange quark on a nucleon appears to be smaller than that of a nonstrange quark by an amount $\Delta$, which can be estimated by

$$\Delta = \sigma_t(\pi^-p) - \sigma_t(K^-p) \tag{1}$$

$$= \sigma_t(\pi^+p) - \sigma_t(K^-n) \tag{2}$$

$$\simeq 3.5\text{–}4 \text{ mb} \tag{3}$$

over the beam momentum range 6–240 GeV/$c$. The difference (1) is illustrated in Fig. 1. Then since the total $NN$ cross section is roughly charge independent,

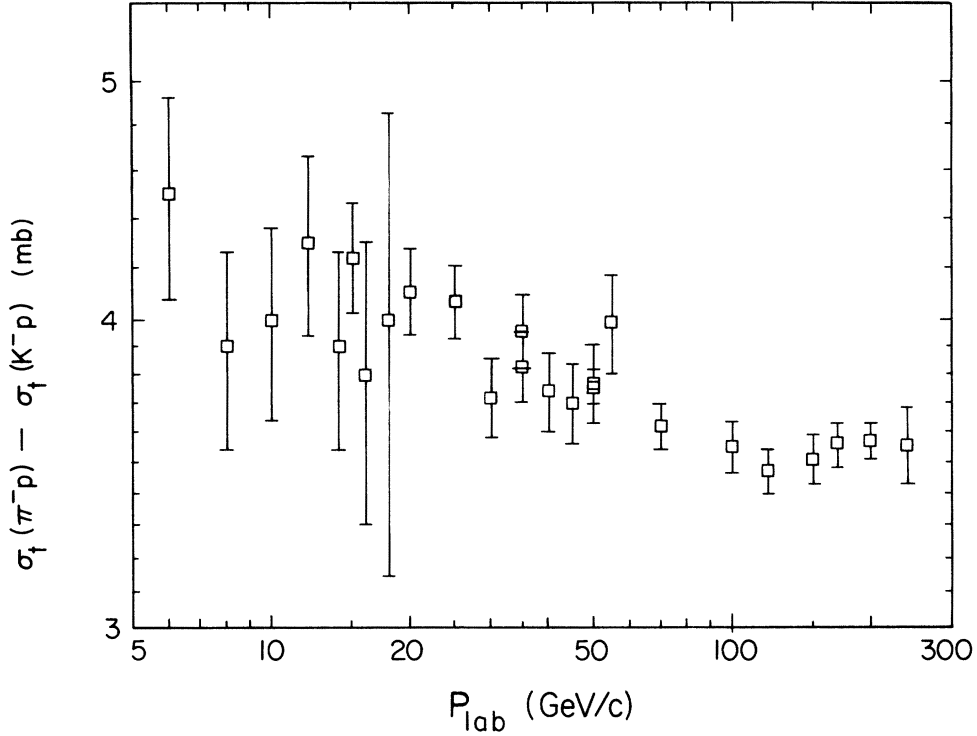$$\sigma_t(pp) \simeq \sigma_t(pn) \equiv \sigma_t(NN), \tag{4}$$

FIG. 1. Difference between $\pi^-p$ and $K^-p$ total cross sections. The data are from Ref. 9.

we have

$$\sigma_t(\Lambda N) \simeq \sigma_t(\Sigma N) = \sigma_t(NN) - \Delta, \tag{5}$$

$$\sigma_t(\Xi N) = \sigma_t(NN) - 2\Delta, \tag{6}$$

$$\sigma_t(\Omega^- N) = \sigma_t(NN) - 3\Delta. \tag{7}$$

Similar "equal-spacing" rules would be expected to hold for total cross sections on deuterons or, for that matter, on any light nucleus.[8] The pre-

dictions of Eqs. (5)–(7) for nucleon and deuteron targets[9] are displayed in Fig. 2.

Some recent measurements of hyperon total cross sections[10-14] are plotted in Fig. 2 and compiled in Table I, along with $NN$ cross sections at similar energies. These measurements are adequate to test the relations (5). With the exception of the surprisingly low values for $\sigma_t(\Sigma^-d)$ and the derived quantity $\sigma_t(\Sigma^-n)$, there is general agree-
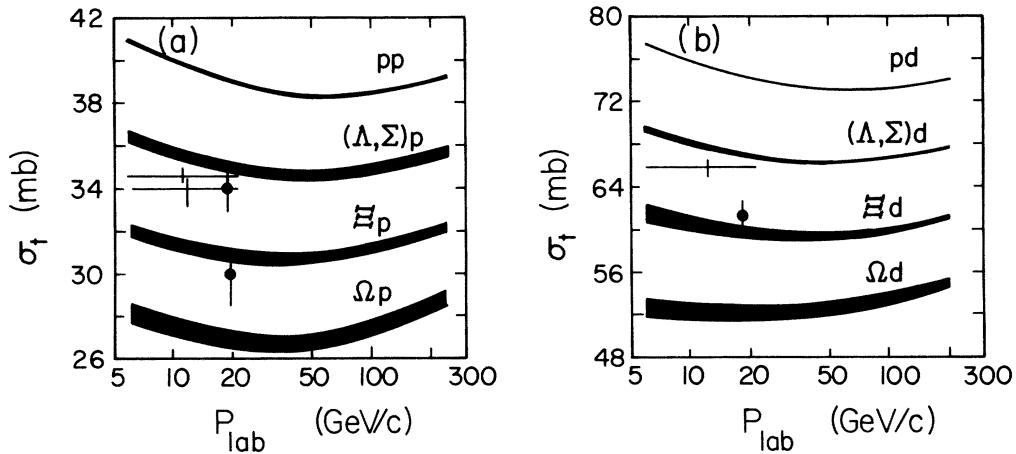


FIG. 2. Additive quark-model predictions for (a) hyperon-nucleon and (b) hyperon-deuteron total cross sections, compared with measurements in $\Lambda$ (+) and $\Sigma^-$ (●) beams. Sources of the data points are given in Table I.

TABLE I.  Hyperon-nucleon total-cross-section values.

| Hyperon $Y$ | Target $A$ | Beam momentum (GeV/$c$) | $\sigma_t(YA)$ (mb) | $\sigma_t(pA)$ (mb) |
|---|---|---|---|---|
| $\Lambda$ | $p$ | 6–21 | $34.6 \pm 0.4$ [a] | $39.10 \pm 0.12$ [b] |
| $\Lambda$ | $d$ | 6–21 | $65.8 \pm 0.8$ [a] | $74.1 \pm 0.7$ [c] |
| $\Lambda$ | $n$ | 6–21 | $34.0 \pm 0.8$ [a,d] | $39.10 \pm 0.12$ [b] |
| $\Sigma^-$ | $p$ | 18.7 | $34.0 \pm 1.1$ [e] | $39.10 \pm 0.12$ [b] |
| $\Sigma^-$ | $d$ | 18.7 | $61.3 \pm 1.4$ [e] | $74.1 \pm 0.7$ [c] |
| $\Sigma^-$ | $n$ | 18.7 | $30.0 \pm 1.2$ [e,d] | $39.10 \pm 0.12$ [b] |

[a] Ref. 10.
[b] Ref. 11; 19 GeV/$c$
[c] Ref. 12; 19 GeV/$c$
[d] Extracted from deuteron target using Glauber correction.
[e] Ref. 13.

ment with the quark-model expectation. Evidently, such tests require the measurement of hyperon-nucleon total cross sections to $\pm 1$ mb.

Whether the quark-model predictions are quantitatively successful remains to be seen. In the similar setting of $\phi N$ scattering, the quark model correctly anticipates that $\sigma_t(\phi N) < \sigma_t(KN)$, but fails numerically, if vector-meson dominance is to believed. The relation

$$\sigma_t(\phi N) = \tfrac{1}{2}[\sigma_t(K^+p) + \sigma_t(K^-p) + \sigma_t(K^+n) + \sigma_t(K^-n)$$
$$- \sigma_t(\pi^+p) - \sigma_t(\pi^-p)] \qquad (8)$$

yields[15,16] $12.85 \pm 0.52$ mb at 6 GeV/$c$ and $13.16 \pm 0.44$ mb at 12 GeV/$c$, whereas the experimental values, deduced from $\phi$ photoproduction,[17] are $8.7 \pm 0.5$ mb at 4.6–6.7 GeV/$c$,[18] $9.3 \pm 0.3$ mb at 8.5 GeV/$c$,[19] $8.7 \pm 0.9$ mb at 9.3 GeV/$c$,[20] and approximately 9.3 mb at 12 GeV/$c$.[21] Hyperon-beam experiments offer the advantage of freedom from the vector-meson-dominance assumption.

If more refined measurements of hyperon-nucleon total cross sections can be made, it will be possible to go beyond qualitative tests of the quark model and investigate the SU(3) structure of the Pomeranchuk trajectory. If SU(3) symmetry holds, the charge-averaged baryon-baryon total cross sections can be written in terms of $t$-channel exchange contributions as

$$\sigma_t(NN) = P_1 + (1 - \alpha/3)P_8 + (1 - \alpha_T/3)f$$
$$- (1 - \alpha_V/3)\omega, \qquad (9)$$

$$\sigma_t(\Lambda N) = P_1 - (2\alpha/3)P_8 + \tfrac{1}{3}(2 - 4\alpha_T/3)f$$
$$- \tfrac{1}{3}(2 - 4\alpha_V/3)\omega, \qquad (10)$$

$$\sigma_t(\Sigma N) = P_1 + (2\alpha/3)P_8 + \tfrac{2}{3}f - \tfrac{2}{3}\omega, \qquad (11)$$

$$\sigma_t(\Xi N) = P_1 - (1 + \alpha/3)P_8 + \tfrac{1}{3}(1 - \alpha_T)f$$
$$- \tfrac{1}{3}(1 - \alpha_V)\omega, \qquad (12)$$

where $P_1$, $P_8$, $f$, and $\omega$ denote suitably normalized contributions of SU(3)-singlet and -octet Pomerons and of ideally mixed $f^0$ and $\omega^0$ trajectories, and $\alpha$, $\alpha_T$, and $\alpha_V$ are the $D/F$ ratios of symmetric to antisymmetric coupling of the octet Pomeron, the tensor-meson trajectories, and the vector-meson trajectories to octet baryons. The singlet couplings of $\omega$ and $f^0$ are chosen to ensure that $\phi$ and $f^*$ decouple from the $\overline{N}N$ vertex.

Equations (9)–(12) permit many interesting exercises. If $\alpha = \alpha_V = \alpha_T = 0$, they reduce to the quark-counting rules (4)–(7) [but without specifying $\Delta$ through Eqs. (1)–(3)]. For any values of $\alpha$, $\alpha_V$, and $\alpha_T$, the cross sections must satisfy a relation similar to the Gell-Mann–Okubo mass formula:

$$\frac{\sigma_t(NN) + \sigma_t(\Xi N)}{2} = \frac{3\sigma_t(\Lambda N) + \sigma_t(\Sigma N)}{4}. \qquad (13)$$

It is usual to assume that baryon-baryon total cross sections are dominated by the Pomeron above an incident momentum of a few GeV/$c$. This assumption is supported by duality considerations,[22-24] and at least roughly by the data. [See Eq. (4) and Fig. 2.] In any case, the $\omega$-exchange contribution can be eliminated by averaging particle and antiparticle cross sections and the $f$-exchange term can be distinguished from the Pomeron by its characteristic energy dependence.[25] If the Pomeron contribution can be isolated, either by assumption or by explicit separation, the ratio $\alpha$ can be extracted from

$$\frac{\sigma_t(NN) - \sigma_t(\Lambda N)}{\sigma_t(NN) - \sigma_t(\Sigma N)} = \frac{1 + \alpha/3}{1 - \alpha}. \qquad (14)$$

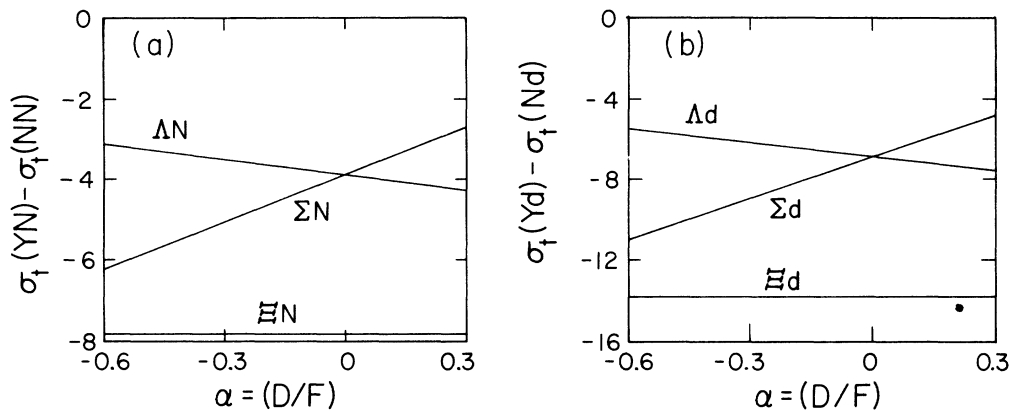The 19-GeV/$c$ data cited in Table I then imply only

FIG. 3. Differences between hyperon and nucleon total cross sections on (a) nucleon and (b) deuteron targets, as functions of the octet coupling parameter $\alpha = D/F$ of the Pomeron, at 50 GeV/$c$. The $\alpha = 0$ values are taken from Fig. 2.

that

$$\alpha \simeq -0.1 \pm 0.2 \quad \text{(nucleon data)}$$

or                                                                                  (15)

$$\alpha \simeq -0.35 \pm 0.10 \quad \text{(deuteron data)}.$$

These values are consistent with zero (the quark-model result) and with another "interesting" value, $\alpha \simeq -0.3$, the $D/F$ ratio of the octet mass-splitting operator.[26]

Let us continue to assume, for illustrative purposes, that at 50 GeV/$c$ the non-Pomeron contributions are negligible. Then, taking the cross-section estimates in Fig. 2 as the values appropriate for $\alpha = 0$, we plot in Fig. 3 the differences $\sigma_t(YN) - \sigma_t(NN)$ as functions of $\alpha = D/F$. A difference of as much as 1.5 mb between $\Lambda N$ and $\Sigma N$ cross sections (or of 3 mb between $\Lambda d$ and $\Sigma d$ cross sections) is quite conceivable. In order to establish this one would have to measure each cross section to an accuracy of 1%.

It is of independent interest to study the energy dependence of $\Lambda N$, $\Sigma N$, $\Xi N$, and $\Omega N$ total cross sections. Do all rise in the same manner as the $pp$ cross section? Does the octet component of vacuum exchange fade away at high energies? (The data in Fig. 1 and the analysis of Ref. 16 indicate that for meson-baryon collisions it does not.)

We now turn to total cross sections of antihyperons on nucleons. In this context it is of interest to discuss the *differences* $\sigma_t(\bar{B}B) - \sigma_t(BB)$. Again, a simple quark-model rule exists for these differences.[24]

Let us define a unit $\delta$ of particle-antiparticle cross-section difference as follows. Count the number of ways an antiquark $\bar{q}_j$ in the projectile antibaryon can annihilate a quark $q_j$ in the target baryon. (See Fig. 4) For each possible annihila-

tion, count one unit $\delta$. Then sum over the quark species $j$. The total contributions (for nucleon and deuteron targets) are listed in Table II, together with numerical estimates at 50 GeV/$c$. To estimate cross-section differences at other momenta, one may use the fact that $\sigma_t(\bar{p}p) - \sigma_t(pp)$ behaves approximately as $p_{lab}^{-0.6}$. To properly test the predictions of Table II at 50 GeV/$c$ requires measurements of total-cross-section differences to within 0.5 mb. Otherwise, the predicted 5:4:3:2:1:0 pattern will be difficult to recognize.

As in the case of baryon-baryon total cross sections, the quark-model predictions just discussed correspond to a particular limit of a more general SU(3) treatment. Again the limit is one of pure $F$-type coupling of the participating Regge-trajectories, which are moreover assumed to be exchange degenerate. The trajectories that govern the total-cross-section differences $\sigma_t(\bar{B}N) - \sigma_t(BN)$ are those of the vector mesons $\omega$ and $\rho$. The SU(3) predictions appropriate for exchange-degenerate vector-meson trajectories are shown in Table III, where the total-cross-section differences are expressed in terms of an overall scale $\delta'$ (presumably proportional to $p_{lab}^{-0.6}$) and the vector-meson $D/F$ ratio $\alpha_V$.

The case $\alpha_V = 0$, as already mentioned, corresponds to the quark-model case ("$\omega^0$-$\rho$ universality"[27]). The differences listed in Table III are
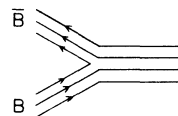


FIG. 4. A contribution to the particle-antiparticle cross-section difference $\sigma_t(\bar{B}B) - \sigma_t(BB)$, according to "Lipkin's rule."

TABLE II. Contributions to the total-cross-section differences $\sigma_t(\bar{B}B) - \sigma_t(BB)$ according to "Lipkin's rule."

| $\Delta\sigma_t$ | Value | 50 GeV/$c$ values (mb) | |
| --- | --- | --- | --- |
| | | Prediction | Experiment |
| $\bar{p}p - pp = \bar{n}n - nn$ | $5\delta$ | $5.72 \pm 0.13$ [a] | $5.72 \pm 0.13$ [b] |
| $\bar{p}n - pn = \bar{n}p - np$ <br> $\Sigma^-p - \Sigma^+p = \bar{\Sigma}^+n - \Sigma^-n$ | $4\delta$ | $4.58 \pm 0.10$ | $4.83 \pm 0.13$ [b] |
| $\bar{\Lambda}N - \Lambda N$ | $3\delta$ | $3.43 \pm 0.08$ | |
| $\Sigma^+p - \Sigma^-p = \bar{\Sigma}^-n - \Sigma^+n$ <br> $\bar{\Xi}^0p - \Xi^0p = \bar{\Xi}^+n - \Xi^-n$ | $2\delta$ | $2.29 \pm 0.05$ | |
| $\bar{\Xi}^+p - \Xi^-p = \bar{\Xi}^0n - \Xi^0n$ | $\delta$ | $1.14 \pm 0.03$ | |
| $\bar{\Omega}^+N - \Omega^-N$ | $0$ | $0$ | |
| $\bar{N}d - Nd$ | $9\delta_d$ | $9.33 \pm 0.22$ [a] | $9.33 \pm 0.22$ [b] |
| $\bar{\Sigma}d - \Sigma d = \bar{\Lambda}d - \Lambda d$ | $6\delta_d$ | $6.22 \pm 0.15$ | |
| $\bar{\Xi}d - \Xi d$ | $3\delta_d$ | $3.11 \pm 0.07$ | |
| $\bar{\Omega}^+d - \Omega^-d$ | $0$ | $0$ | |

[a] Input.
[b] Carroll et al., Ref. 9.

plotted as functions of $\alpha_V$ in Fig. 5, for 50 GeV/$c$. The measured $\bar{p}n$-$pn$ total-cross-section difference, which is also plotted in Fig. 5(a), implies that

$$-0.4 \lesssim \alpha_V \lesssim 0.1. \tag{16}$$

The $\bar{p}n$-$pn$ information at other energies is no more restrictive.

Independent information on $\alpha_V$ comes from differences between pairs of meson-nucleon total cross sections. As will be shown in Sec. VI,

$$\alpha_V = 1 - \frac{2[\sigma_t(K^-n) - \sigma_t(K^+n)]}{[\sigma_t(K^-p) - \sigma_t(K^+p)]}, \tag{17}$$

providing the $\rho$ and $\omega^0$ trajectories are degenerate. This quantity is plotted as a function of beam momentum in Fig. 6(a). Similarly, the combination

$$\alpha_V = \frac{2[\sigma_t(\pi^-p) - \sigma_t(\pi^+p)]}{[\sigma_t(K^-p) - \sigma_t(K^+p)]} - 1, \tag{18}$$

derived under the same assumptions, is plotted in Fig. 6(b). The systematic increase of $\alpha_V$ at high momenta in Fig. 6(b) is a direct consequence of the observed splitting[28] of the $\rho$ and $\omega$ intercepts. In meson-nucleon scattering, the parameter $\alpha_V$ can only be determined by combinations which mix $\omega$ and $\rho$ contributions.

However, hyperon beams permit $\alpha_V$ to be measured by combinations of cross sections which only involve $\omega$ exchange. These are the baryon-antibaryon cross-section differences on deuterons already discussed, or the charge-averaged differ-

ences on nucleons. The quark-model predictions, known as $\omega$-universality relations,[27] are

$$\Delta\sigma_t(NN) = \tfrac{3}{2}\Delta\sigma_t(\Lambda N) = \tfrac{3}{2}\Delta\sigma_t(\Sigma N)$$
$$= 3\Delta\sigma_t(\Xi N) = 3\Delta\sigma_t(KN), \tag{19}$$

and similarly for deuteron targets. These are illustrated in Fig. 7. The general SU(3) symmetry relations can be read off from the deuteron entries in Table III, or from Fig. 5(b). Measurement of, for example, the quantities $\sigma_t(\bar{\Lambda}d) - \sigma_t(\Lambda d)$ and $\sigma_t(\bar{\Sigma}d) - \sigma_t(\Sigma d)$ to $\pm\tfrac{1}{3}$ mb at 50 GeV/$c$ would repre-

TABLE III. SU(3)-invariance relations for total-cross-section differences.

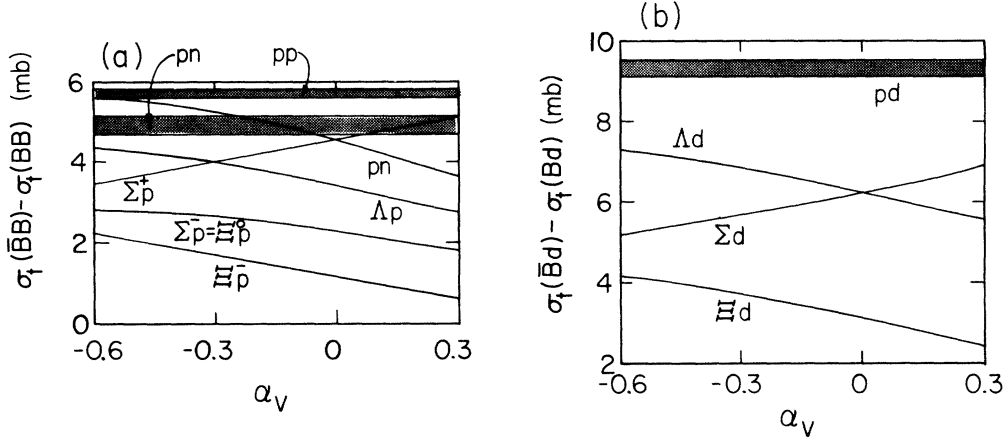| $\Delta\sigma_t$ | Value predicted by SU(3) |
| --- | --- |
| $\bar{p}p - pp = \bar{n}n - nn$ | $4\delta'[1 + (1 - \alpha_V)^2/4]$ |
| $\bar{p}n - pn = \bar{n}p - np$ | $4\delta'(1 - \alpha_V)$ |
| $\Sigma^-p - \Sigma^+p = \bar{\Sigma}^+n - \Sigma^-n$ | $4\delta'$ |
| $\bar{\Lambda}N - \Lambda N$ | $3\delta'(1 - \alpha_V/3)(1 - 2\alpha_V/3)$ |
| $\Sigma^+p - \Sigma^-p = \bar{\Sigma}^-n - \Sigma^+n$ <br> $\bar{\Xi}^0p - \Xi^0p = \bar{\Xi}^+n - \Xi^-n$ | $2\delta'(1 - \alpha_V)$ |
| $\bar{\Xi}^+p - \Xi^-p = \bar{\Xi}^0n - \Xi^0n$ | $\delta'(1 - \alpha_V)^2$ |
| $\bar{p}d - pd$ | $3\delta'_d(1 - \alpha_V/3)$ |
| $\bar{\Lambda}d - \Lambda d$ | $2\delta'_d(1 - 2\alpha_V/3)$ |
| $\bar{\Sigma}d - \Sigma d$ | $2\delta'_d$ |
| $\bar{\Xi}d - \Xi d$ | $\delta'_d(1 - \alpha_V)$ |

FIG. 5. Baryon-antibaryon total-cross-section differences on (a) nucleon and (b) deuteron targets, as functions of the coupling parameter $\alpha_V = D/F$ for the vector-meson trajectories, at 50 GeV/$c$. The $\rho$ and $\omega^0$ trajectories are assumed to be exchange-degenerate for the nucleon-target predictions. Experimental data, shown as shaded bands, are from Carroll *et al.*, Ref. 9.

sent an important new contribution to knowledge of the vector-meson couplings. The measurement of a full set of $\omega$-exchange contributions will permit the same sort of test of SU(3) invariance as has been made in the past[29] using relative rates of hyperon resonance decays.

### III. ELASTIC SCATTERING

The real parts of forward elastic scattering amplitudes are expected to display simple regularities similar to those just discussed for total

cross sections. In an exchange-degenerate picture, the forward nonflip spin-averaged elastic scattering amplitude can be written in terms of Regge-pole contributions as

$$\left.\begin{array}{c} A[\overline{B}B] \\ A[BB] \end{array}\right\} = A_{\text{Pomeron}} + |R(p_{\text{lab}})| \{i - \cot[\pi\alpha(0)/2]$$

$$\pm (i + \tan[\pi\alpha(0)/2])\}.$$

(20)

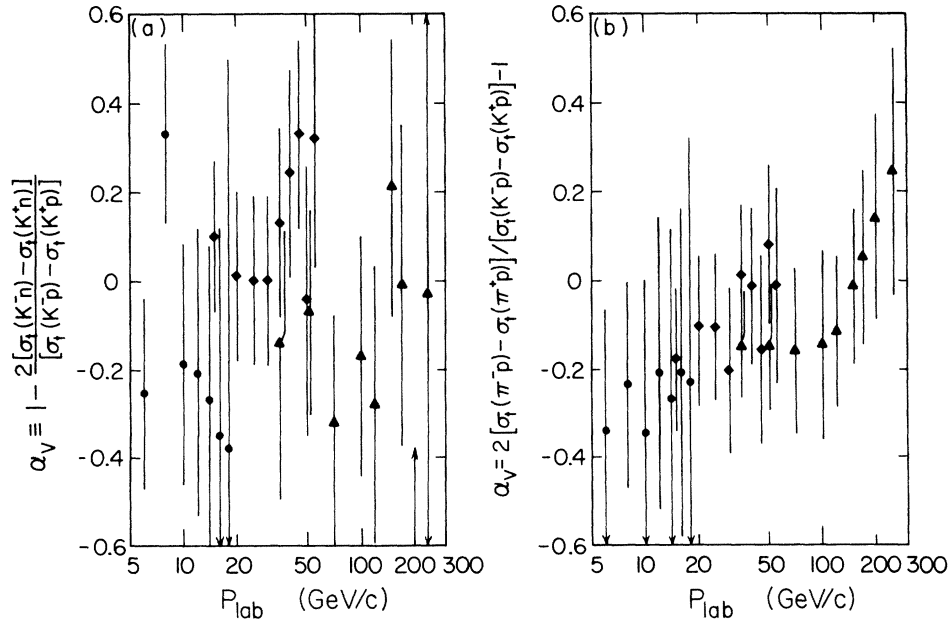The first term in brackets refers to the tensor



FIG. 6. (a) Experimental information on the vector-meson coupling parameter $\alpha_V$, defined by Eq. (17). (b) Experimental values of $\alpha_V$ as defined by Eq. (18). The data are from Ref. 9.

trajectories, and the second to the vector trajec-
tories. Approximating the common intercept as
$\alpha(0) = \frac{1}{2}$, we find

$$A[\bar{B}B] \simeq A_P + 2i|R|, \tag{21}$$

and

$$A[BB] \simeq A_P - 2|R|, \tag{22}$$

so that the non-Pomeron real part in $BB$ scatter-
ing is the negative of the non-Pomeron imaginary
part in $\bar{B}B$ scattering. More explicitly, we may
write

$$\text{Re}A[\bar{B}B] - \text{Re}A[BB] = \text{Im}A[\bar{B}B] - \text{Im}A[BB] \tag{23}$$

or

$$\frac{\text{Re}A[\bar{B}B]}{\text{Im}A[BB]} - \frac{\text{Re}A[BB]}{\text{Im}A[BB]} = \frac{\sigma_t(\bar{B}B) - \sigma_t(BB)}{\sigma_t(BB)}, \tag{24}$$

which may be rearranged to read

$$\rho_{BB} = \frac{\text{Re}A[BB]}{\text{Im}A[BB]}$$

$$= \frac{\text{Re}A_P}{\text{Im}A_P} - \frac{\sigma_t(\bar{B}B) - \sigma_t(BB)}{\sigma_t(BB)}. \tag{25}$$

The predictions of Sec. II for total cross sections
also, therefore, predict non-Pomeron contribu-
tions to real parts of forward elastic amplitudes.

As an illustration, we may calculate these con-
tributions using the quark-model predictions[24] for
cross-section differences. Our expectations for
50 GeV/$c$ are shown in Table IV, along with experi-
mental values for the ratio Re/Im in $pp$ scattering.[30]
It is expected that the term $\text{Re}A_P/\text{Im}A_P$ in (25)
should be very nearly the same for all baryon pro-
jectiles. (This contribution should be given, in the
present approximation, by the differences between
the second and third columns in Table IV.) Con-
sequently, measurements of real to imaginary
parts with precision of a few percent at 50 GeV/$c$
will aid in testing the systematics of Regge-pole
amplitudes. A possible example of real-part ef-
fects has already appeared at much lower energies.
In the incident-momentum range 1–4 GeV/$c$, it
has been observed[31] that $\sigma_{\text{elastic}}(\Sigma^+p) > \sigma_{\text{elastic}}(\Sigma^-p)$.
This inequality may be due to the larger real part
to be expected in the $\Sigma^+p$ amplitude, as indicated
in Table IV.

We can make additional predictions for the real-
to-imaginary ratio by applying the derivative an-
alyticity relations[32] to our predictions for total
cross sections. The curves plotted in Fig. 8 were
computed by fixing the crossing-even amplitudes
from that in $pp$ scattering according to Eqs. (1)
and (5)–(7) and the crossing-odd amplitudes from
that in $pp$ scattering [compare Fig. 7(a)] according
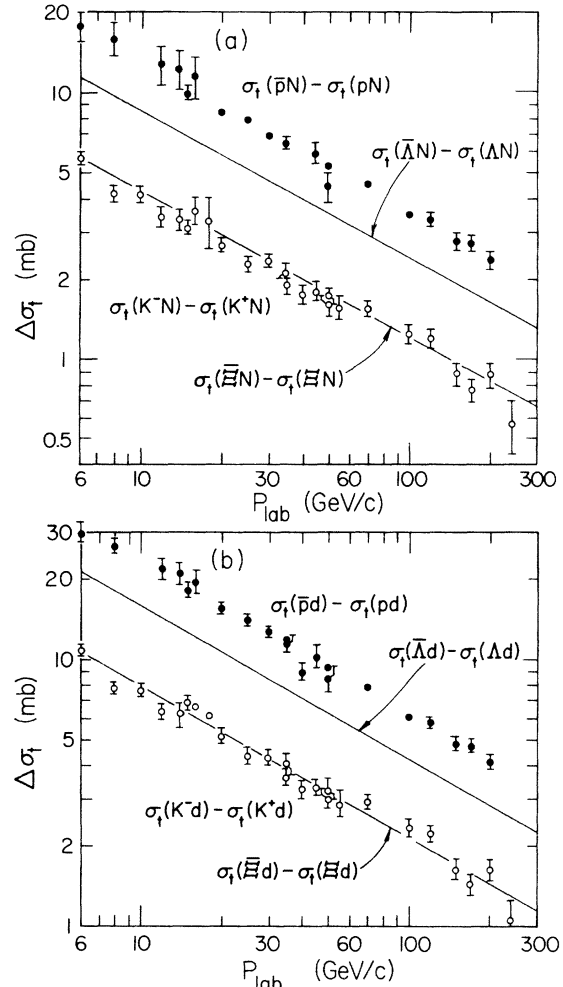to the $\omega$-universality relations (19). (See also Ta-



FIG. 7. (a) The $\omega$-exchange contributions to total-cross-
section differences on nucleon targets. Solid lines are
the predictions of the $\omega$-universality relations (19).
(b) Same for deuteron targets. The data are from Ref.
9. The $\Lambda$-beam expectations apply for $\Sigma$ beams as well,
in both (a) and (b).

TABLE IV. Non-Pomeron contributions to real parts
of forward elastic hyperon-nucleon scattering amplitudes
at 50 GeV/$c$.

| Process | $(\text{Re/Im})_{\text{non-Pomeron}}$ [a] | $(\text{Re/Im})_{\text{expt}}$ |
|---------|---------------------------|-------------------------------|
| $pp$ | $-0.15$ | $-0.157 \pm 0.012$ [b] |
|      |         | $-0.159 \pm 0.030$ [c] |
| $\Sigma^+p$ | $-0.13$ | |
| $\Sigma^-p$ | $-0.07$ | |
| $\Xi^-p$ | $-0.04$ | |
| $\Omega^-p$ | $0$ | |

[a] $(\text{Re/Im})_{\text{non-Pomeron}}$ is expected to behave roughly as
$p_{\text{lab}}^{-1/2}$.
[b] Bartenev et al., Ref. 30, at 51.5 GeV.
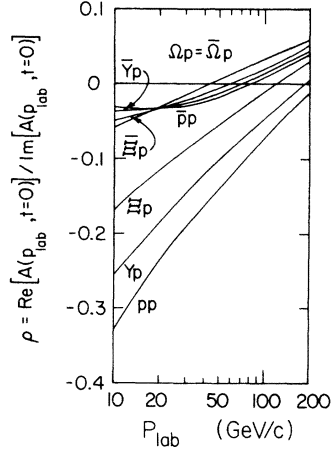[c] Beznogikh et al., Ref. 30, at 50.63 GeV/$c$.

FIG. 8. *Charge-average* predictions for the ratio of real to imaginary parts of forward elastic scattering amplitudes in hyperon-proton collisions, compared to predictions for $pp$ and $\bar{p}p$ scattering. The symbol $Y$ represents both $\Lambda$ and $\Sigma$ projectiles.

ble III.) From these expectations, we verify that the interesting level of precision is a few percent at 50 GeV/$c$.

The logarithmic slopes $b$ of differential cross sections $d\sigma/dt = Ae^{bt}$ reflect geometrical information complementary to that provided by total cross sections. For an absorbing disk of fixed opacity, the quantity $b/\sigma_t$ is independent of the size of the disk. Empirically,[33] it appears that in the hundred-GeV/$c$ regime $b$ is more nearly proportional to $\sigma_t^{1/2}$. (See Fig. 9.) This corresponds to reduced opacity for the smaller hadron-proton total cross sections.[34] The extreme case of $\psi$ ($J$)-nucleon scattering involves a total cross section about $\frac{1}{40}$ the $pp$ total cross section but a slope only 4–6 times smaller.[35]

Using the relation

$$b = (1.027 \text{ GeV}^{-1})\sqrt{\sigma_t} \qquad (26)$$

suggested by the 100-GeV/$c$ data in Fig. 9 and the quark-model predictions for total cross sections described in Sec. II, we are led to expect

$$\frac{b(\bar{\Lambda}p)}{b(pp)} = \frac{b(\bar{\Sigma}p)}{b(pp)} \simeq 0.99,$$

$$\frac{b(\Lambda p)}{b(pp)} = \frac{b(\Sigma p)}{b(pp)} \simeq 0.96,$$

$$\frac{b(\bar{\Xi}p)}{b(pp)} \simeq 0.93, \qquad (27)$$

$$\frac{b(\Xi p)}{b(pp)} \simeq 0.91,$$

$$\frac{b(\Omega p)}{b(pp)} = \frac{b(\bar{\Omega}p)}{b(pp)} \simeq 0.86$$

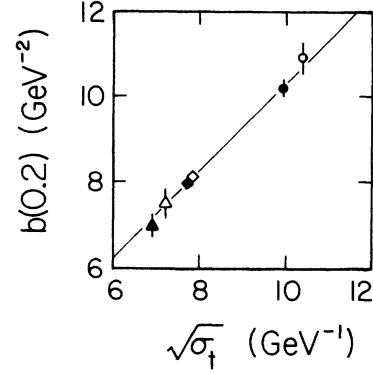in the 50–200-GeV/$c$ regime. If instead the con-



FIG. 9. Comparison of

$$b\,(0.2) \equiv \left.\frac{\partial(\ln d\sigma/dt)}{\partial|t|}\right|_{|t| = 0.2 \,(\text{GeV}/c)^2}$$

with $\sqrt{\sigma_t}$ for 100-GeV/$c$ $\pi^+p$ ($\blacklozenge$), $\pi^-p$ ($\Diamond$), $K^+p$ ($\blacktriangle$), $K^-p$ ($\triangle$), $pp$ ($\bullet$), and $\bar{p}p$ ($\bigcirc$) collisions. The data are from Ref. 33. The straight line is $b = (1.027 \text{ GeV}^{-1})\sqrt{\sigma_t}$.

nection

$$b = C \cdot \sigma_t \qquad (28)$$

applies, these ratios should differ from unity by twice as much.

At 18.7 GeV/$c$, Blaising *et al.*[36] have reported

$$b(\Sigma^-p)/b(pp) = 0.93 \pm 0.055, \qquad (29)$$

$$\sigma_t(\Sigma^-p)/\sigma_t(pp) = 0.87 \pm 0.03, \qquad (30)$$

$$[\sigma_t(\Sigma^-p)/\sigma_t(pp)]^{1/2} = 0.93 \pm 0.02, \qquad (31)$$

supporting the view that $b(\Sigma p) < b(pp)$, but not distinguishing between the functional forms of (26) and (28). Such a distinction is of interest since it allows one to determine whether reduced hyperon-nucleon total cross sections are simply geometrical size effects or (as we suspect) indications of reduced opacity associated with the scattering of strange particles. The 23.3-GeV/$c$ measurements of $\Sigma^-p$ and $\Xi^-p$ elastic scattering by Némethy *et al.*[37] and the 1–17-GeV/$c$ study of $\Lambda p$ elastic scattering by Anderson *et al.*[38] also indicate that hyperon-proton elastic scattering is less collimated than proton-proton elastic scattering.

If elastic hyperon-nucleon scattering can be studied at $|t|$ values as high as 1–2 (GeV/$c$)$^2$, there is another important question that such experiments can answer. Proton-proton scattering in this $|t|$ interval shows a strong energy dependence: A deep dip develops as $p_{\text{lab}}$ is increased from 100 to 200 GeV/$c$.[39] This dip could be due to properties of the Pomeron itself, or could reflect interference of the Pomeron with non-Pomeron trajectories. One would expect hyperon-nucleon scattering to behave similarly in the first case, and not so similarly in the second. (As we have mentioned, the

non-Pomeron contributions to baryon-baryon scattering are much more widely differing than the Pomeron contributions.)

## IV. DIFFRACTION DISSOCIATION

In any diffractive process that involves a pion in the final diffracted state, the Deck effect[40] plays an important role. This role is somewhat diminished in processes that involve kaons, because of the larger kaon mass.

The process

$$\Sigma^- + A \rightarrow \pi^- + \Lambda + A \tag{32}$$

has been studied at Brookhaven.[41] The dominant effect seems to be a clustering of events at low effective $\Lambda\pi^-$ mass. No resonant behavior was seen at small $|t|$. In principle such a process allows one to extract the $\Sigma^- \rightarrow \Lambda\pi^-$ coupling constant.[42] This constant is usually extracted (very imprecisely) from dispersion relations for $\overline{K}N \rightarrow \Lambda\pi$. It is needed to test SU(3) and to determine that $D/F$ ratio for the coupling of pseudoscalar mesons to the baryon octet. Similar considerations apply to the processes

$$\Sigma + A \rightarrow \Sigma + \pi + A, \tag{33}$$

$$\Lambda + A \rightarrow \Sigma + \pi + A, \tag{34}$$

$$\Xi + A \rightarrow \Xi + \pi + A. \tag{35}$$

It is notable that the $\Xi\Xi\pi$ coupling is expected to be very much smaller than the $NN\pi$ coupling. Both SU(6) and fits to hyperon $\beta$ decay using the Cabibbo theory (with partial conservation of axial-vector current to relate axial currents to pseudoscalar mesons)[43] predict $(D/F)_{\text{pseudoscalars}} \simeq \frac{3}{2}$, so that

$$\frac{g^2(\Xi^- \rightarrow \Xi^0\pi^-)}{g^2(n \rightarrow p\pi^-)} = \frac{(D-F)^2}{(D+F)^2} = \frac{1}{25}. \tag{36}$$

Hence the Deck effect may be considerably suppressed in diffraction of a $\Xi^-$ beam. It will also be suppressed in diffraction of an $\Omega^-$ beam since the transition $\Omega \rightarrow \Omega\pi$ is forbidden.

One can expect diffraction of hyperons to produce a number of resonances that have not yet been observed. Figure 10, taken with minor modifications from Ref. 4, shows states corresponding to likely SU(6) multiplets. The circled entries are those that could be produced using hyperon beams if the Gribov-Morrison selection rule[44]

$$\Delta P = (-1)^{\Delta J} \tag{37}$$

held. We have also assumed that the Pomeron is an SU(3) singlet. In this case the missing states of Fig. 10 that could be observed are (a) the ra-

dial excitations of the hyperons, belonging to $56'$, $L = 0$, (b) certain $\frac{3}{2}^-$ states in the $\underline{70}$ multiplet,[45] and (c) $\Omega^{-*}$ states of $J^P = \frac{3}{2}^+$ and $\frac{7}{2}^+$ belonging to the $\underline{56}$, $L = 2$ multiplet. All of the $\Omega^{-*}$ states should be above $\Xi\overline{K}$ threshold; the mass scale in Fig. 10 is not meant to be interpreted literally. Mass predictions are given in Table V. They are obtained from masses of observed states[46] simply by adding 100 to 150 MeV for each unit of negative strangeness. The $\Omega^{-*}$ states look the most promising: (i) as mentioned, the $\Omega^-$ should not lead to a Deck effect associated with pions; (ii) there are at least four $\Omega^{-*}$ states expected to be produced diffractively between $\Xi\overline{K}$ threshold (1800 MeV) and 2350 MeV. This compensates somewhat for the expected low $\Omega^-$ intensities. Next most promising are the $\Xi^*$ states, since these (like the $\Omega^{-*}$'s) cannot be produced in the direct channel, and as mentioned may not be subject to a very strong Deck background.

[*Note added in proof.* The preliminary data of Ref. 42 indicate some production of $\Sigma(1385)$ in $\Sigma^- + A \rightarrow \Lambda^0 + \pi^- + X$ for $|t| > 0.1$ GeV/$c$. If this effect is due to Pomeron exchange, it violates both (37) and the assumption of an SU(3)-singlet Pomeron. Measurements at various energies will be required to distinguish Pomeron exchange from exchange of ordinary Regge trajectories such as $f_0$ or $\omega$, which are expected to have octet contributions.]

Resonances belonging to the $\underline{20}$ of SU(6) cannot be produced in the direct channel since the product

$$\underline{35} \otimes \underline{56} = \underline{56} \oplus \underline{70} \oplus \underline{700} \oplus \underline{1134} \tag{38}$$

does not contain $\underline{20}$. In quark-model language, single-quark transitions cannot take a totally symmetric $\underline{56}$ into a totally antisymmetric $\underline{20}$. If diffraction is a single-quark-transition process, states in the $\underline{20}$ cannot be produced diffractively starting with a $\underline{56}$ projectile like $\Lambda$, $\Sigma$, $\Xi$, or $\Omega$. On the other hand, it has been suggested[47] that Pomeron exchange is really two-gluon exchange. If so, diffraction easily could excite a *pair* of quarks, as assumed in Ref. 2.

The $\underline{20}$ contains $(8,2) \oplus (1,4)$. In the harmonic-oscillator quark model one expects a $\underline{20}$, $L = 1$, $N = 2$ roughly degenerate with the $\underline{56}$, $L = 2$ or perhaps slightly higher.[48] This would contain octets with $J^P = \frac{1}{2}^+$ and $\frac{3}{2}^+$, and singlets ($\Lambda$'s) with $J^P = \frac{1}{2}^+, \frac{3}{2}^+, \frac{5}{2}^+$. The $\underline{20}$ is expected to couple to $\underline{35} \otimes \underline{70}$ since

$$\underline{35} \otimes \underline{70} = \underline{20} \oplus \underline{56} \oplus \underline{70} \oplus \underline{70} \oplus \underline{540} \oplus \underline{560} \oplus \underline{1134}. \tag{39}$$

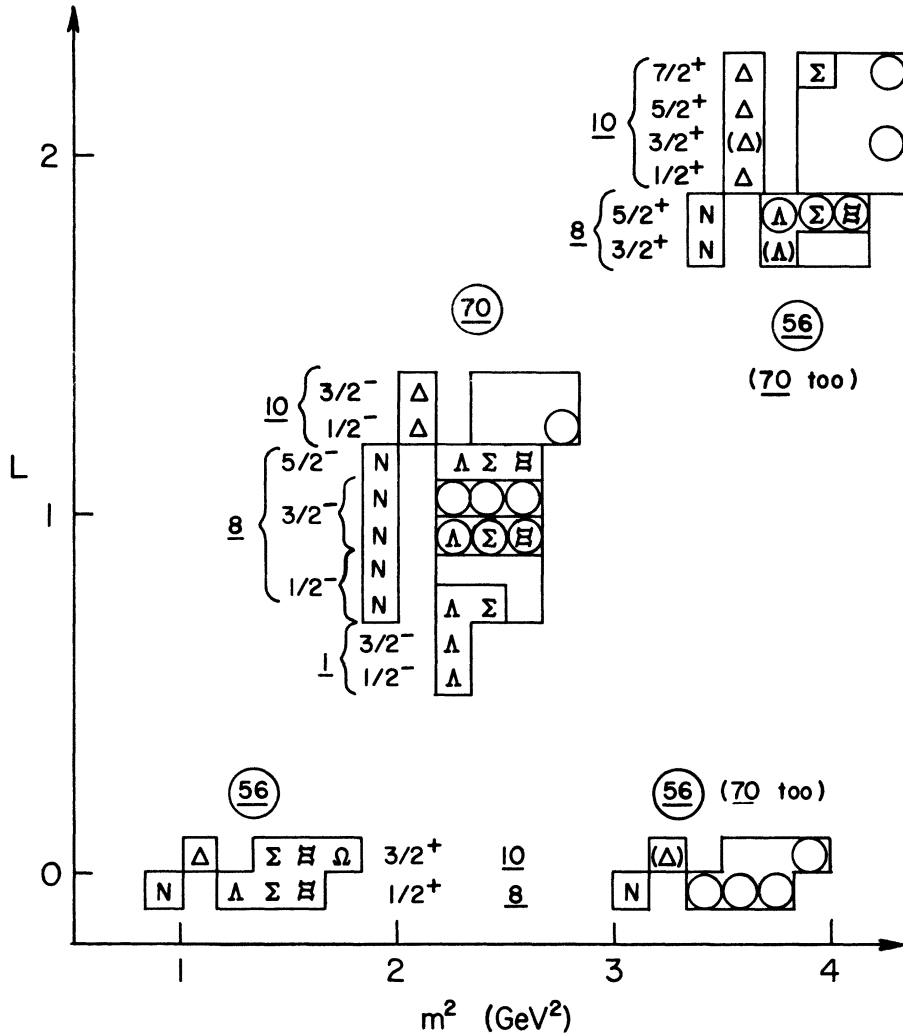Hypothetical production and decay schemes would

FIG. 10. "Box score" for filling the major multiplets of $SU(6) \otimes O(3)$ with observed baryons. The mass scale is very rough. Mixing among states is possible; in this case the assignments to specific $SU(3)$ representations are educated guesses based on masses and couplings. Blank states enclosed in heavy lines denote missing states. States with the same $(I, Y)$ are listed vertically; those with the same $J^P$ are listed horizontally. Circled entries are states that could be produced by diffractive excitation of hyperon beams if (37) holds and if the Pomeron is an $SU(3)$ singlet.

then be, for example,

$$\Lambda + A \to \Lambda^*(\tfrac{1}{2}^+ \text{ or } \tfrac{5}{2}^+) + A$$
$$\searrow \Sigma^*(\text{in } \underline{70}) + \pi$$
$$\searrow \Lambda\pi, \Sigma\pi, N\overline{K}. \tag{40}$$

The signal for $\underline{20}$ production would be the absence in the $\Lambda\pi\pi$, $\Sigma\pi\pi$, or $N\overline{K}\pi$ final states of any two-body resonances belonging to the baryon $\underline{56}$ or the meson $\underline{35}$. It is important to study states of more than two bodies if $\underline{20}$'s are to be seen. The existence or nonexistence of $\underline{20}$'s continues to be a topic of strong debate among theorists, and an experimental solution to the problem would be most welcome.

A very exotic possibility would be to study the dissociation of hyperons into a charmed meson and a charmed baryon. This process is discussed further in Sec. IX.

### V. CHARGE AND HYPERCHARGE EXCHANGE

Field and Quigg have compiled detailed predictions for these processes.[6] Here we content ourselves with a few simple observations.

(a) Isospin relates the reactions $\Lambda p \to \Sigma^+ n$ and $\Sigma^- p \to \Lambda n$. (The processes are time-reversed isospin reflections of one another.)

(b) If $t$-channel flip amplitudes are dominant, with $D/F \simeq 3/2$, the exchange of $\pi$, $\rho$, and $A_2$ gives

$$\frac{\Lambda p \to \Sigma^+ n}{np \to pn} = \frac{2}{3}\left(\frac{D}{D+F}\right)^2 \simeq \frac{1}{4}, \tag{41}$$

$$\frac{\Sigma^- p \to \Sigma^0 n}{np \to pn} = 2\left(\frac{F}{D+F}\right)^2 \simeq \frac{1}{3}, \tag{42}$$

$$\frac{\bar{\Lambda}p \to \bar{\Sigma}^+ n}{\bar{p}p \to \bar{n}n} = \frac{2}{3}\left(\frac{D}{D+F}\right)^2 \simeq \frac{1}{4}. \tag{43}$$

In practice the nonflip $\rho$ and $A_2$ amplitudes contribute substantially to process (42), though not to (41) or (43).[6] (Nonflip $\rho$ and $A_2$ couplings are probably mostly $F$-type.) Hence a one-pion-exchange peak survives in (41) and (43) up to 400 GeV/$c$, but is washed out above 100 GeV/$c$ in (42). By passing to small $|t|$, it may be possible to extract the $\Lambda\Sigma\pi$ and $\Sigma\Sigma\pi$ couplings from (41)–(43). This would be very helpful for performing the SU(3) and SU(6) tests mentioned in Sec. IV.

(c) There are many possible hypercharge-exchange reactions that can be studied using hyperon beams. These include $\Lambda p \to p\Lambda$, $\Xi^- p \to \Lambda\Lambda$, $\Omega^- n \to \Xi^- \Lambda$, and others. The latter two are particularly amusing since they involve two hyperons in the final state, the decays of which analyze their polarizations. All the hypercharge-exchange reactions related by SU(3) to $np \to pn$ or $\bar{p}p \to \bar{n}n$ appear to be of the same order as these last two[6]; there are no drastic suppressions because of the variety of amplitudes that can contribute.

It should be noted that there are already at one's disposal certain hypercharge-exchange reactions in baryon-antibaryon scattering: The processes $\bar{p}p \to \bar{\Lambda}\Lambda, \bar{\Sigma}\Sigma, \bar{\Lambda}\Sigma^0, \bar{\Sigma}^0\Lambda$ have been studied with low statistics in bubble chambers up to 7 GeV/$c$.[49] It would certainly be worthwhile to extend such reactions to higher energies and higher statistics using multiparticle spectrometers and both hydrogen and deuterium targets, especially if it is possible to make line-reversal comparisons with hyperon-initiated reactions.

(d) Exotic exchange already has been studied below 7 GeV/$c$ in $\bar{p}p \to \bar{\Sigma}^+\Sigma^-$ and $\bar{p}p \to \bar{Y}_1^{*+}Y_1^{*-}$.[49] The exotic exchange cross section seems to fall off with $s$ roughly as $s^{-8}$. It would be useful to study reactions such as

$$\bar{p}p \to \bar{\Sigma}^+\Sigma^-, \tag{44}$$

$$\bar{p}p \to \bar{\Xi}^+\Xi^- \tag{45}$$

in multiparticle spectrometers. On the other hand, the related reactions

$$\Sigma^- p \to p\Sigma^-, \tag{46}$$

$$\Xi^- p \to p\Xi^- \tag{47}$$

may actually be easier to measure if hyperon

TABLE V. Hyperon states belonging to likely SU(6) multiplets that may be produced diffractively from hyperon beams. The rule (37) is assumed, and the Pomeron is taken to be an SU(3) singlet. Mixing of states with members of other SU(3) representations is neglected.

| SU(6) multiplet | (SU(3), SU(2)) | $J^P$ | State (mass) |
|---|---|---|---|
| $\underline{56}, L = 0$ | (8, 2) | $\frac{1}{2}^+$ | $\Lambda(1570\text{–}1620)$ [a,b] |
| | | | $\Sigma(1570\text{–}1620)$ [a,c] |
| | | | $\Xi(1670\text{–}1770)$ [a] |
| | (10, 4) | $\frac{3}{2}^+$ | $\Omega(2000\text{–}2150)$ [d] |
| $\underline{70}, L = 1$ | (8, 2) | $\frac{3}{2}^-$ | $\Lambda(1690)$ [e] |
| | | | $\Sigma(1660)$ [e] |
| | | | $\Xi(1820)$ [e] |
| | (8, 4) [f] | $\frac{3}{2}^-$ | $\Lambda(1800\text{–}1850)$ [g] |
| | | | $\Sigma(1800\text{–}1850)$ [g] |
| | | | $\Xi(1900\text{–}2000)$ [g] |
| | (10, 2) [f] | $\frac{1}{2}^-$ | $\Omega(1950\text{–}2100)$ [h] |
| $\underline{56}, L = 2$ | (8, 2) | $\frac{5}{2}^+$ | $\Lambda(1815)$ [e] |
| | | | $\Sigma(1915)$ [e] |
| | | | $\Xi(2030)$ [e] |
| | (10, 4) | $\left\{ \begin{matrix} \frac{3}{2}^+ \\ \frac{7}{2}^+ \end{matrix} \right\}$ | $\Omega(2200\text{–}2350)$ [i] |

[a] Based on $N(1470)$.
[b] May have been observed at 1750 MeV (see Ref. 46), or at 1565 MeV (see Ref. 52).
[c] May have been observed at 1620–1640 MeV (see Refs. 46, 52).
[d] Based on $\Delta(1690)$ (see Ref. 46).
[e] Established.
[f] May be forbidden if quark spin is conserved in diffraction.
[g] Based on $N(1700)$ (see Ref. 46). $\Lambda$ may have been observed at 1840 MeV; $\Sigma$ may have been observed at 1840 or 1912 MeV (see Ref. 52).
[h] Based on $\Delta(1650)$.
[i] Based on $\Delta(1950)$ and on probable absence of large spin-orbit splittings.

beams turn out to be as intense as now contemplated.

## VI. MISSING $\Lambda^*, \Sigma^*, \Xi^*$ STATES

In this section we shall make an estimate based on SU(3) and on two-component duality[50,51] for the average resonance contribution to all elastic $0^- $-$\frac{1}{2}^+$ channels. This is done by calculating the exchange-degenerate $t$-channel tensor- and vector-exchange contributions to $\sigma_t$ and then equating their sum to the average resonant contribution $\bar{\sigma}_R$. These contributions are shown in Table VI. They imply a large number of relations between observed elastic channels such as $\bar{K}N$ and unobserved elastic ones such as $\pi\Sigma$ or $\pi\Lambda$. Let us decompose the $\pi\Sigma$ and $\bar{K}N$ channels into isospin amplitudes:

$$\bar{\sigma}_R(K^-p) = \frac{1}{2}\bar{\sigma}_R(\bar{K}N, I=0) + \frac{1}{2}\bar{\sigma}_R(\bar{K}N, I=1), \tag{48a}$$

$$\bar{\sigma}_R(K^-n) = \bar{\sigma}_R(\bar{K}N, I=1), \tag{48b}$$

TABLE VI. Non-Pomeron contributions to $\sigma_t(0^- \frac{1}{2}^+)$ in SU(3) limit. Entries underlined involve exchange-degenerate $f'$-$\phi$ exchange; others involve $f_0$-$A_2$-$\omega$-$\rho$ exchange. The underlined entries **may** correspond to suppressed contributions because of the lower $f'$-$\phi$ intercept.

| $0^- \backslash \frac{1}{2}^+$ | $p$ | $n$ | $\Lambda$ | $\Sigma^+$ | $\Sigma^0$ | $\Sigma^-$ | $\Xi^0$ | $\Xi^-$ |
|---|---|---|---|---|---|---|---|---|
| $\pi^+$ | $F-D$ | $2F$ | $F-\frac{5}{3}D$ | $0$ | $F$ | $2F$ | $0$ | $F-D$ |
| $\pi^0$ | $\frac{1}{2}(3F-D)$ | | $F-\frac{2}{3}D$ | | $F$ | | $\frac{1}{2}(F-D)$ | |
| $\pi^-$ | $2F$ | $F-D$ | $F-\frac{5}{3}D$ | $2F$ | $F$ | $0$ | $F-D$ | $0$ |
| $\eta$ | $\frac{1}{2}F-\frac{1}{6}D$ | | $\frac{1}{3}(F-\frac{5}{3}D)+\frac{5}{3}(F+\frac{1}{3}D)$ | | $\frac{1}{3}F+\frac{5}{3}(F-D)$ | | $\frac{1}{6}(F-D)+\frac{5}{3}(2F)$ | |
| $K^+$ | $0$ | | $F+\frac{1}{3}D$ | $F-D$ | | | $2F$ | |
| $K^0$ | $0$ | | $F+\frac{1}{3}D$ | $F-D$ | | | $2F$ | |
| $\bar{K}^0$ | $F-D$ | $2F$ | $F-\frac{5}{3}D$ | $0$ | $F$ | $2F$ | $0$ | $F-D$ |
| $K^-$ | $2F$ | $F-D$ | $F-\frac{2}{3}D$ | $2F$ | $F$ | $0$ | $F-D$ | $0$ |

$$\bar{\sigma}_R(\pi^-\Sigma^+) = \tfrac{1}{2}\bar{\sigma}_R(\pi\Sigma, I=1) + \tfrac{1}{3}\bar{\sigma}_R(\pi\Sigma, I=0), \qquad (48c)$$

$$\bar{\sigma}_R(\pi^0\Sigma^+) = \tfrac{1}{2}\bar{\sigma}_R(\pi\Sigma, I=1). \qquad (48d)$$

Then

$$\bar{\sigma}_R(\bar{K}N, I=1) = F - D, \qquad (49a)$$

$$\bar{\sigma}_R(\bar{K}N, I=0) = 3F + D, \qquad (49b)$$

$$\bar{\sigma}_R(\pi\Sigma, I=1) = 2F, \qquad (49c)$$

$$\bar{\sigma}_R(\pi\Sigma, I=0) = 3F. \qquad (49d)$$

Then the $\pi\Sigma$ and $\pi\Lambda$ channels may be expressed in terms of the $\bar{K}N$ ones as

$$\bar{\sigma}_R(\pi\Lambda) = \tfrac{3}{4}\bar{\sigma}_R(\bar{K}N, I=1) + \tfrac{1}{12}\bar{\sigma}_R(\bar{K}N, I=0), \qquad (50)$$

$$\bar{\sigma}_R(\pi\Sigma, I=1) = \tfrac{1}{2}\bar{\sigma}_R(\bar{K}N, I=1) + \tfrac{1}{2}\bar{\sigma}_R(\bar{K}N, I=0), \qquad (51)$$

$$\bar{\sigma}_R(\pi\Sigma, I=0) = \tfrac{3}{4}\bar{\sigma}_R(\bar{K}N, I=1) + \tfrac{3}{4}\bar{\sigma}_R(\bar{K}N, I=0). \qquad (52)$$

We have chosen to express these channels in terms of others of the same strangeness only because the level densities are then roughly comparable. Table VI also shows, for example, that $\bar{\sigma}_R(\pi^+p)$ $=\bar{\sigma}_R(\pi^+\Xi^-)$. The former channel has a few large $\Delta$ contributions coming from 10's, while the latter is expected to have a number of smaller $\Xi^*$ contributions from direct-channel 10's *and* 8's.

These relations are illustrated in Figs. 11(a)–11(d). A clear "deficiency" is seen in all three $\pi Y$ channels, especially if only the "established" resonances of Ref. 46 are used. The situation is improved somewhat by the more speculative set of

Ref. 52. In each case, the average resonant cross section in the $\pi Y$ channel is only about 60% of that in the $\bar{K}N$ counterpart. There is, however, no guarantee that the same resonances which couple strongly to $\bar{K}N$ also couple strongly to $\pi\Lambda$ or $\pi\Sigma$. In fact, experience has shown us that when physical states mix with one another (as in the $K^0$-$\bar{K}^0$ system) the eigenstates of the mass matrix tend to have very different couplings to physical channels. Such mixing is to be expected among quark-model states.[53-56] One specific example is a predicted $\Lambda(\sim 1800, \frac{1}{2}^-)$, expected to decouple from $\bar{K}N$ and to have a width of roughly 400 MeV into $\pi\Sigma$.[53,54]

The obvious solution would be to study $\pi$-$\Lambda$ or $\pi$-$\Sigma$ elastic scattering.[4] With the advent of hyperon beams, this may not be as farfetched as it sounds. The reactions illustrated in Fig. 12 can be studied in multiparticle spectrometers. They should prove to be fruitful sources of new resonances even if one-pion exchange cannot be separated completely from $\rho$ or $A_2$ exchange.

It goes without saying that all the $\Xi^*$ channels are very "deficient." Up to now, $\Xi^*$'s have been produced by baryon exchange with incident $K^-$. The $\Xi^*$'s seen in this way are those which couple strongly to $\bar{K}\Lambda$ or $\bar{K}\Sigma$. In a reaction such as

$$\Xi^- + p \to \Xi^{*0} + n \qquad (53)$$

one is much more likely to see the $\Xi^*$'s that couple strongly to $\Xi\pi$. This may be a very different set of $\Xi^*$'s from those already observed.
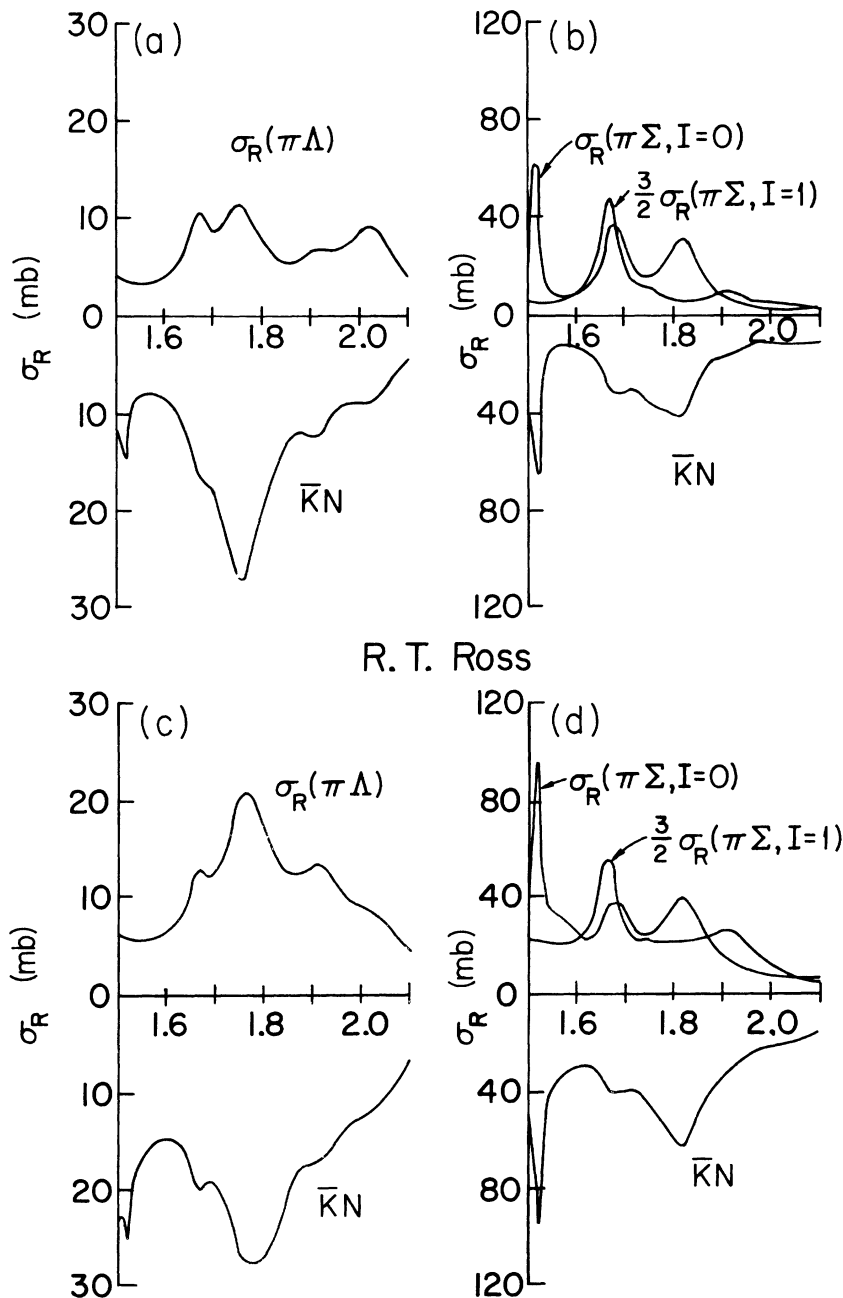
FIG. 11. Tests of the relations (50)–(52). Resonance parameters are taken from Ref. 46 [(a), (b)], or from Table 2 of Ross, Ref. 52 [(c), (d)]. The curves labeled $\overline{K}N$ are in (a) and (c) the right-hand side of Eq. (50), and in (b) and (d) the right-hand side of Eq. (52) as functions of $E_{c.m.}$ (in GeV). If relations (50)–(52) hold, the upper and lower curves on each figure should be equal on average. A deficiency in the known $\pi Y$ resonances is apparent in all three channels, according to both compilations of $Y^*$ parameters.

An independent estimate of "resonance deficiencies" may be made using Adler-Weisberger relations of the type discussed by Gilman and Harari.[57] We illustrate this for the $\pi\Sigma$ case. A clear-cut "deficiency" occurs in the $\pi\Sigma$ Adler-Weisberger relation:

$$(g_A^\Lambda)^2 + (g_A^\Sigma)^2 + \frac{f_\pi^2}{\pi} \int_{\nu_0}^\infty \frac{d\nu}{\nu}[\sigma_t^{\pi^-\Sigma^+}(\nu) - \sigma_t^{\pi^+\Sigma^+}(\nu)] = 2;$$

$$\nu \equiv (s - m_\Sigma^2 - m_\pi^2); \quad f_\pi = 135 \text{ MeV}. \quad (54)$$

If the integral is cut off at $E_{c.m.} = 1700$ MeV, the left-hand side is 1.40 [for $(D/F)_{0-\frac{1}{2}+\frac{1}{2}+} = \frac{3}{2}$]. The observed $\pi\Sigma$ resonances above 1700 MeV add very little to this sum: For example, the increment from the states listed in Ref. 46 in the range 1700–2000 MeV/$c^2$ is only about 0.02. The $\Sigma(2030, \frac{7}{2}^+)$ and $\Lambda(2100, \frac{7}{2}^-)$ each account for less than 0.01.

The *average* cross-section difference in Eq. (54), according to Table VI, may be estimated using

$$\bar\sigma_t^{\pi^-\Sigma^+}(\nu) - \bar\sigma_t^{\pi^+\Sigma^+}(\nu) = \bar\sigma_t^{K^-p}(\nu) - \bar\sigma_t^{K^+p}(\nu),$$

$$\simeq \bar\sigma_1(\nu_1/\nu)^{1/2}, \quad (55)$$

where $\sigma_1$ is the value of the difference at some value $\nu_1$.[58] From the $K^\pm p$ data quoted in Ref. 46, one estimates $\sigma_1 \simeq 20$ mb at $\nu_1 = 0.72$ GeV$^2$ (corresponding to $E_{c.m.}^{\pi\Sigma} = 1.7$ GeV). The contribution of the "Regge tail" to the sum rule (54) above $E_{c.m.} = 1.7$ GeV is then estimated to be

$$\frac{f_\pi^2}{\pi} \int_{0.72}^\infty \frac{d\nu}{\nu}[\sigma_t^{\pi^-\Sigma^+} - \sigma_t^{\pi^+\Sigma^+}] = 0.58. \quad (56)$$

Together with the contribution below 1.7 GeV of 1.40, this saturates the sum rule (54). Hence the use of Table VI to estimate missing contributions to *sum rules* may not be a bad approximation. It is interesting that the range $1.7 \text{ GeV} \leqslant E_{c.m.} \leqslant 2.2$ GeV should contribute roughly 35% of Eq. (56), or 0.20. As mentioned, the observed $\pi\Sigma$ resonances[46] in this range fall short of this expected contribution by at least a factor of 5. This means either that semi-local resonance saturation is a poor approximation, or that there are many $\pi\Sigma$ resonances in this range awaiting discovery. Similarly, from (56) and Table VI, one expects

$$\frac{f_\pi^2}{\pi} \int_{0.72}^\infty \frac{d\nu}{\nu}(\sigma_t^{\pi^+\Xi^-} - \sigma_t^{\pi^-\Xi^-}) = 0.58\left(\frac{1 - \alpha_V}{2}\right)$$

$$= 0.29 \text{ if } \alpha_V = 0;$$

$$= 0.39 \text{ if } \alpha_V = -\frac{1}{3}. \quad (57)$$

(For $\pi\Xi$ scattering, $\nu = 0.72$ corresponds to $E_{c.m.} \simeq 1.8$ GeV.) Again, 35% of Eq. (57) should come from the lowest 500 MeV in the center-of-mass energy. The observed $\Xi$ states in this range come
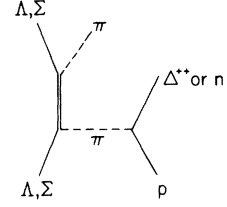


FIG. 12. Reactions for investigating the resonance contributions to pion-hyperon total cross sections.

nowhere near saturating the sum rule semilocally. A quantitative estimate cannot be made, however, since we lack information on spin parity and on branching ratios for most of these states.

## VII. HADRONIC EXPERIMENTS WITH POLARIZED HYPERON BEAMS

In $p$-Be collisions at Fermilab, the $\Lambda$'s produced at $p_\perp = 1.5$ GeV/$c$ are 25% polarized for a wide range of values of $p_\parallel$.[7] These polarized $\Lambda$'s are produced at some cost in intensity, as the production cross section is peaked at $p_\perp = 0$. Nontheless, these polarized hyperons will be used for a measurement of the $\Lambda$ magnetic moment,[59] and one can imagine several uses for them in hadronic experiments as well.

If high-energy inelastic collisions produce polarized particles, the collisions of these particles in turn should be expected to produce asymmetries in inclusive reactions. [In the inclusive reactions of polarized protons at much lower energies (6 GeV/$c$) these asymmetries have turned out to be surprisingly large.[60]]

The charge- and hypercharge-exchange reactions mentioned in Sec. V would be much better understood if they could be initiated with polarized hyperons. The same is true for the diffractive processes mentioned in Sec. IV and the one-pion-exchange processes noted in Sec. VI. On the other hand, the polarization effects on elastic scattering (Sec. III) and total cross sections (Sec. II) are not expected to be very large.

## VIII. COULOMB DISSOCIATION OF HYPERONS

This subject already has been discussed by Lipkin[2]; results are presented here for completeness. A $\Lambda$ beam will permit the study of $\Sigma^0 \to \Lambda\gamma$ using the Primakoff effect. This process already has been measured at CERN,[61] yielding the lifetime

$$\tau_{\Sigma^0} = (0.62 \pm 0.15) \times 10^{-19} \text{ sec}. \quad (58)$$

This is to be compared with the value based on SU(3):

$$\tau_{\Sigma^0} = 0.8 \times 10^{-19} \text{ sec}. \quad (59)$$

The processes $\Xi^{*-} \to \Xi^{-}\gamma$ and $Y^{*-} \to \Sigma^{-}\gamma$ are forbidden by $U$ spin.[2,62] The rates for the processes $Y_1^{*+} \to \Sigma^{+}\gamma$ and $\Delta^{+} \to p\gamma$ are *equal*, by $U$ spin.[63] SU(3) implies $\bar{\Gamma}(Y_1^{*0} \to \Lambda\gamma) = \frac{3}{4}\bar{\Gamma}(Y_1^{*+} \to \Sigma^{+}\gamma)$.[63] Finally, SU(6) implies[63]

$$\bar{\Gamma}(Y_1^{*0} \to \Lambda\gamma) = \bar{\Gamma}(\Sigma^0 \to \Lambda\gamma). \tag{60}$$

In fact, since the Primakoff rates scale as $(2J+1)\tilde{\bar{\Gamma}}$ for production of a spin-$J$ particle, and since $Y_1^{*0} \to \Lambda\pi^0$ is the dominant decay of $Y_1^{*0}$, Eq. (60) implies that a considerable background in

$$\Lambda + Z \to \Sigma^0 + Z \tag{61}$$
$$\searrow$$
$$\Lambda\gamma$$

could in principle arise from

$$\Lambda + Z \to Y_1^{*0} + Z \tag{62}$$
$$\searrow$$
$$\Lambda\pi^0$$

especially at high energies where the $Y_1^{*0}$ production is not significantly suppressed by kinematics.

## IX. PRODUCTION OF "NEW" PARTICLES; HIGH-$p_\perp$ PROCESSES

If charmed baryons exist,[64] it may be possible to produce them in several types of hadronic reactions. An example is associated production, e.g.,

$$\pi^-(\bar{u}d) + p(uud) \to (\bar{c}d)^- + (udc)^+. \tag{63}$$

Here $c$ is the charmed quark, assumed to have charge $\frac{2}{3}$. Similar reactions are possible, of course, in theories with more than one heavy quark.

It has been argued[65] that reaction (63) may be suppressed because it involves charm exchange. A similar but perhaps not identical process would be the diffractive excitation of a nucleon into an $N^*$, followed by its subsequent decay into charmed particles[66,67]:

$$N + A \to N^* + A \tag{64}$$
$$\searrow$$
$$B_c + M_c.$$

To produce baryons which are both charmed and strange one might use a reaction such as

$$K^-(s\bar{u}) + p(uud) \to (\bar{c}d)^- + (cus)^+. \tag{65}$$

Unfortunately, this involves the exchange of a particle which is not only charmed but exotic $(cs\bar{u}d)$ as well. An analog of reaction (64) using a hyperon beam which presents no such problems is

$$\Lambda + A \to \Lambda^*(uds) + A \tag{66}$$
$$\searrow$$
$$(usc)^+ + (\bar{c}d)^-.$$

If one used a $\Xi$ beam one could even produce baryons with $S = -2$ and $C = 1$; e.g.,

$$\Xi^- + A \to \Xi^{*-}(dss) + A$$
$$\searrow$$
$$(css)^0 + (\bar{c}d)^-. \tag{67}$$

Such baryons would be very difficult to produce in any other way.

These processes (and related ones in the central region of rapidity space) become less far-fetched when one realizes that hyperon beams may prove to be *the most intense $S < 0$ beams at high energies*.[68] In this context hyperon beams may also be very worthwhile in investigating the role of strange quarks in high-transverse-momentum phenomena. One expects inclusive $K^-$ production by $\Sigma^-$ to be appreciable, even at high $p_\perp$, if the basic process involves the hard scattering of quarks in the $\Sigma^-$.

## X. CONCLUSIONS

Some quantitative expectations have been given for hadronic experiments with hyperon beams. Measurements of $\sigma_t(\Lambda N)$, $\sigma_t(\Sigma N)$, $\sigma_t(\Xi N)$, and $\sigma_t(\Omega N)$ to a few percent will be useful in checking quark-model predictions. If measurements of the first two or three can be performed to an accuracy of $1\%$, one can determine in addition the $D/F$ ratio in the octet Pomeron coupling to octet baryons. Similarly, measurements of $\sigma_t(\bar{Y}N) - \sigma_t(YN)$ $(Y = \Lambda, \Sigma, \Xi, \Omega)$ to $\pm\frac{1}{3}$ mb will allow meaningful checks of the quark model and measurement of the $D/F$ ratio in the $(\omega, \rho)$ octet coupling to octet baryons. In elastic-scattering experiments, measurements of the ratios $\rho$ of real to imaginary parts of forward amplitudes will provide additional information on couplings of non-Pomeron trajectories if these measurements can be carried out to $\pm 0.02$. Slopes in elastic scattering should display the ordering $b(\Omega^-p) < b(\Xi p) < b(\Sigma p) \approx b(\Lambda p) < b(pp)$, since empirically $b^2 \propto \sigma_t$. Measurements of $d\sigma/dt$ at high $|t|[|t| \simeq 1$ (GeV/$c$)$^2]$ can reveal whether non-Pomeron trajectories or "optical" considerations are responsible for a deep energy-dependent dip seen in $pp$ scattering at this $|t|$ value.

Diffraction of $\Lambda$ and $\Sigma$ hyperon beams can be useful for studying pion-hyperon couplings by the Deck effect. It has been argued that the Deck effect should be greatly suppressed in the diffractive scattering of $\Xi^-$ and $\Omega^-$, and diffractively produced resonances should correspondingly play a relatively larger role. (There are also the greatest number of "missing" resonances predicted by the quark model in these channels.) Ways of identifying a diffractively produced $\underline{20}$ of SU(6) have been identified.

Some simple uses of charge-exchange and hyper-charge-exchange reactions have been discussed. These included tests of isospin and SU(3), isolation of pion-hyperon couplings, amplitude analyses,

and exotic-exchange studies. Related processes could be studied using $\bar{p}p \to$ hyperon + antihyperon, but hyperon beams are expected to be more intense than $\bar{p}$ beams at most energies,[68] and in certain cases the final states will be considerably simpler. (Compare $\bar{p}p \to \bar{\Sigma}\Sigma$ with $\Sigma p \to p\Sigma$, for example.)

It has been shown that SU(3) for exchanged trajectories implies substantial non-Pomeron contributions to total cross sections in nonexotic channels such as $\pi^-\Sigma^+$, $\pi^+\Xi^-$, etc. In turn, these are expected to be reflected in direct-channel resonant contributions. At present, large deficiencies in these contributions exist, particularly in the channels $\pi\Lambda$, $\pi\Sigma$ ($I=1$), and $\pi\Xi$. Hyperon-pion scattering is suggested as a possible remedy for this deficiency.

Some suggestions have been made for hadron physics with polarized hyperon beams: Inclusive reactions look particularly promising, though the studies of any processes which involved detailed spin analysis (such as resonance production by diffraction or one-pion exchange) could benefit greatly from the use of polarized incident hyperons.

We have summarized some SU(3) and SU(6) predictions for Coulomb dissociation of hyperons and conclude that $\Lambda \to Y_1^{*0}$ presents a potential background in the study of $\Lambda \to \Sigma^0$ at high energies.

Hyperon beams also may be useful in producing baryons which are both charmed and strange and in studying inclusive processes, particularly those at high transverse momentum.

In summary, hadron physics with hyperon beams presents a wide range of opportunities for interesting experiments. These include symmetry tests, searches for missing quark-model states, searches for fundamentally new particles, and all the other experiments that benefit by having a variety of incident beams. It is not unreasonable to expect that by roughly doubling this variety (as hyperon beams will allow us to do) we should understand hadron physics considerably more thoroughly.

## ACKNOWLEDGMENTS

---

*Work supported in part by the Alfred P. Sloan Foundation; also at Enrico Fermi Institute, University of Chicago, Chicago, Illinois 60637.

†Operated by Universities Research Association Inc. under contract with the Energy Research and Development Administration.

‡Work supported in part by U. S. Energy Research and Development Administration under Contract No. ER-(11-1)-1764.

[1]J.-M. Gaillard and M. K. Gaillard, "Non-Leptonic Interactions," Chap. IV of *Weak Interactions*, edited by M. K. Gaillard, a volume in the series *Textbook on Elementary Particle Physics*, edited by M. Nikolic (Institut National de Physique Nucléaire et de la Physique des Particles, Paris, to be published).

[2]H. J. Lipkin, Phys. Rev. D 7, 846 (1973); in *Particles and Fields–1975*, proceedings of the meeting of the APS Division of Particles and Fields, Seattle, edited by H. J. Lubatti and P. M. Mockett (University of Washington, Seattle, Washington, 1976), p. 352; H. J. Lipkin, in Proceedings of the XI Rencontre de Moriond, Flaine, France, 1976, edited by J. Tran Thanh Van (to be published).

[3]J. J. Kubis and H. R. O. Walters, Nucl. Phys. B17, 547 (1970).

[4]J. L. Rosner, Phys. Rep. 11C, 189 (1974).

[5]J. L. Rosner, in Argonne Report No. ANL-HEP-CP-7558, edited by E. L. Berger and S. L. Kramer (unpublished), p. 165.

[6]R. D. Field and C. Quigg, Fermilab Report No. FERMI-LAB-Pub-76/35-THY (unpublished).

[7]L. Pondrom, private communication. See also Devlin, Ref. 14, and G. Bunce *et al.*, Phys. Rev. Lett. 36, 1113 (1976).

[8]H. J. Lipkin, Phys. Rev. 174, 2151 (1968).

[9]The $\pi$, $K$, and $p$ beam data are taken from W. Galbraith *et al.*, Phys. Rev. 138, B913 (1965); K. J. Foley *et al.*, Phys. Rev. Lett. 19, 330 (1967); 19, 857 (1967); S. P. Denisov *et al.*, Phys. Lett. 36B, 415 (1971); 36B, 528 (1971); Nucl. Phys. B65, 1 (1973); A. S. Carroll *et al.*, Phys. Rev. Lett. 33, 928 (1974); 33, 932 (1974); Phys. Lett. 61B, 303 (1976).

[10]S. Gjesdal *et al.*, Phys. Lett. 40B, 152 (1972).

[11]K. J. Foley *et al.*, Phys. Rev. Lett. 19, 857 (1967).

[12]G. Bellettini *et al.*, Phys. Lett. 19, 341 (1965).

[13]J. Badier *et al.*, Phys. Lett. 41B, 387 (1972).

[14]T. J. Devlin (Rutgers-Michigan-Wisconsin Collaboration), Bull. Am. Phys. Soc. 21, 93 (1976), abstract JB5.

[15]The $\pi N$ and $KN$ data are from Ref. 9. For an up-to-date plot of the right-hand side of Eq. (8), see Fig. 7 of Ref. 16.

[16]C. Quigg and E. Rabinovici, Phys. Rev. D 13, 2525 (1976).

[17]We have neglected the real part of the $\phi N$ forward scattering amplitude and used the vector-meson-dominance relation

$$\sigma_t^2(\phi p) = (64\pi\gamma_\phi^2/4\pi\alpha)d\sigma(\gamma N \to \phi N)/dt|_{t=0},$$

with

$$\gamma_\phi^2/4\pi = 2.82 \pm 0.17,$$

a weighted average of storage-ring values given in

Ref. 18.

[18]H.-J. Behrend et al., Phys. Lett. 56B, 409 (1975).

[19]C. Berger et al., Phys. Lett. 39B, 659 (1972).

[20]J. Ballam et al., Phys. Rev. D 7, 3150 (1973).

[21]R. L. Anderson et al., Phys. Rev. Lett. 30, 149 (1973).

[22]J. L. Rosner, Phys. Rev. Lett. 21, 950 (1968); 21, 1422(E) (1968).

[23]H. J. Lipkin, Nucl. Phys. B9, 349 (1969).

[24]H. J. Lipkin, Phys. Rev. Lett. 16, 1015 (1966).

[25]We are assuming, in the spirit of conventional Regge-pole phenomenology, that the Pomeron and $f^0$ are distinct objects. If the Pomeron and $f^0$ are to be identified, as suggested by C. Rosenzweig and G. F. Chew, Phys. Lett. 58B, 93 (1975), a different SU(3) analysis is required.

[26]Relations analogous to (9)—(14) can be written not only for nucleon and deuteron targets, but also for any targets (such as light nuclei) to which the Pomeron can be assumed to couple in a factorizable manner.

[27]P. G. O. Freund, Phys. Rev. Lett. 15, 929 (1965).

[28]For a compendium of Reggeon intercepts, see C. Quigg, in Particles and Fields—1975 (Ref. 2), p. 1.

[29]See, for example, R. D. Tripp, in Proceedings of the XIV International Conference on High Energy Physics, Vienna, edited by J. Prentki and J. Steinberger (CERN, Geneva, 1968), p. 171.

[30]V. Bartenev et al., Phys. Rev. Lett. 31, 1367 (1973); G. Beznogikh et al., Phys. Lett. 39B, 411 (1972).

[31]G. R. Charlton et al., Phys. Lett. 32B, 720 (1970).

[32]J. B. Bronzan, in Argonne Report No. ANL/HEP 7327 (unpublished), p. 33. A lucid pedagogical discussion of this technique for computing $\rho$ is given by J. D. Jackson, in Phenomenology of Particles at High Energies, edited by R. L. Crawford and R. Jennings (Academic, New York, 1974), p. 2. An up-to-date comparison with data on the ratio $\rho_{\bar{p}p}$ appears in C. Quigg, Ref. 28. A related method was used in a slightly different physical context by D. A. Geffen, Phys. Rev. 112, 1370 (1958).

[33]Fermilab Single Arm Spectrometer Collaboration, Phys. Rev. Lett. 35, 1195 (1975). This relation has been noticed by V. Barger and R. J. N. Phillips, Nucl. Phys. B97, 452 (1975).

[34]See, for example, A. W. Chao and C. N. Yang, Phys. Rev. D 8, 2063 (1973). We are grateful to E. Rabinovici for discussions on this general topic.

[35]D. Nease, thesis, Cornell University, 1976 (unpublished).

[36]J. J. Blaising et al., Phys. Lett. 58B, 121 (1975).

[37]P. Nemethy et al., in Particles and Fields—1975 (Ref. 2), p. 335.

[38]K. J. Anderson et al., Phys. Rev. D 11, 473 (1975).

[39]C. W. Akerlof et al., Phys. Lett. 59B, 197 (1975).

[40]R. T. Deck, Phys. Rev. Lett. 13, 169 (1964).

[41]V. Hungerbühler et al., Phys. Rev. D 10, 2051 (1974).

[42]The reaction $n + A \rightarrow p + \pi^- + A$ serves as calibration. [Note added in proof. Preliminary data from the BNL hyperon beam experiment of the BNL—Pittsburgh—University of Massachusetts collaboration for the reaction $\Sigma^- + A \rightarrow (\Sigma^0, \Lambda^0) + X$ have been analyzed in the triple-Regge formalism to yield $(g_{\Sigma\Sigma\pi}^2 + g_{\Lambda\Sigma\pi}^2)/g_{nn\pi}^2 = 0.9 \pm 0.3$. This is to be compared to the SU(3) prediction of 1.12. See W. E. Cleland, in Proceedings of the XI Rencontre de Moriond, Flaine, France, 1976, edited by J. Tran Thanh Van (to be published)].

[43]K. Kleinknecht, in Proceedings of the XVII Internation-

al Conference on High Energy Physics, London, 1974, edited by J. R. Smith (Rutherford Lab, Chilton, Didcot, Berkshire, England, 1974), p. III-23, gives the value $(D/F)_{0^-} = 1.92 \pm 0.08$.

[44]D. R. O. Morrison, Phys. Rev. 165, 1699 (1968). This rule follows from angular momentum conservation in the forward direction but lacks a theoretical justification for $\theta \neq 0°$. If [as suggested by the data of Yu. M. Antipov et al., Nucl. Phys. B63, 153 (1973)] Pomeron exchange is important in the reaction $\pi^- p \rightarrow A_2^- p$, the rule fails. Alternative selection rules have been advanced by T. T. Chou and C. N. Yang [Phys. Rev. 175, 832 (1968)] and by R. Carlitz, S. Frautschi, and G. Zweig [Phys. Rev. Lett. 23, 1134 (1969)].

[45]The missing $\Lambda$, $\Sigma$, and $\Xi$ with $J^P = \frac{3}{2}^-$ in the 70, $L = 1$ are expected to have quark spin $\frac{3}{2}$. They may be difficult to produce diffractively if quark spin is conserved in diffractive processes.

[46]Particle Data Group, Phys. Lett. 50B, 1 (1974). (Note added in proof. A new Review of Particle Properties [Particle Data Group, Rev. Mod. Phys. 48, S1 (1976)], which contains revised parameters for several $Y^*$'s and one new state, $\Lambda$ (1860), has appeared. We have reevaluated the sum rules (50)—(52) using the new parameters. The most substantial change is a doubling of $\bar{\sigma}_R(\pi\Lambda)$ near 1915 MeV. Our conclusions about the overall deficiency of $\pi Y$ resonances are unaffected, however.)

[47]F. E. Low, Phys. Rev. D 12, 163 (1975).

[48]Some evidence for an $N^*$ belonging to a 20, with mass around 2 GeV, has been claimed by D. Yaffe et al., in Baryon Resonances—73, proceedings of the Purdue Conference, edited by E. C. Fowler (Purdue Univ. Press, West Lafayette, Indiana, 1973), p. 85.

[49]B. Sadoulet, CERN-HERA Report No. 69-2 (unpublished); H. W. Atherton et al., Nucl. Phys. B29, 477 (1971).

[50]P. G. O. Freund, Phys. Rev. Lett. 20, 235 (1968).

[51]H. Harari, Phys. Rev. Lett. 20, 1395 (1968).

[52]R. T. Ross, Rutherford Laboratory Report No. RL-75-115 (unpublished), presented at the EPS International Conference on High Energy Physics, Palermo.

[53]D. Faiman and D. E. Plane, Nucl. Phys. B50, 379 (1972).

[54]W. Petersen and J. L. Rosner, Phys. Rev. D 6, 820 (1972).

[55]A. J. G. Hey, P. J. Litchfield, and R. J. Cashmore, Nucl. Phys. B95, 516 (1975).

[56]D. Faiman, private communication. See also D. Faiman, in proceedings of the Workshop on Theoretical Physics, Erice, 1974 (unpublished).

[57]F. Gilman and H. Harari, Phys. Rev. 165, 1803 (1968).

[58]At low energies there is some ambiguity regarding the variable in which to compare the two sides of (55). We choose the crossing-symmetric variable $\nu$ for simplicity.

[59]G. Bunce et al., Fermilab Approved Experiment No. E-440, 1975 (unpublished).

[60]A. Lesnik et al., Phys. Rev. Lett. 35, 770 (1975); M. Marshak, private communication.

[61]F. Dydak et al. CERN-Dortmund-Heidelberg report, 1976 (unpublished).

[62]G. L. Kane, Acta Phys. Polon. B3, 845 (1972).

[63]We neglect kinematic corrections and use $\bar{\Gamma}$ to represent a partial width before such corrections are applied.

[64]S. L. Glashow, J. Iliopoulos, and L. Maiani, Phys. Rev. D $\underline{2}$, 1285 (1970).

[65]R. D. Field and C. Quigg, Fermilab Report No. FERMILAB-75/15-THY (unpublished).

[66]G. Snow, Nucl. Phys. $\underline{B55}$, 445 (1973).

[67]M. K. Gaillard, B. W. Lee, and J. L. Rosner, Rev. Mod. Phys. $\underline{47}$, 277 (1975).

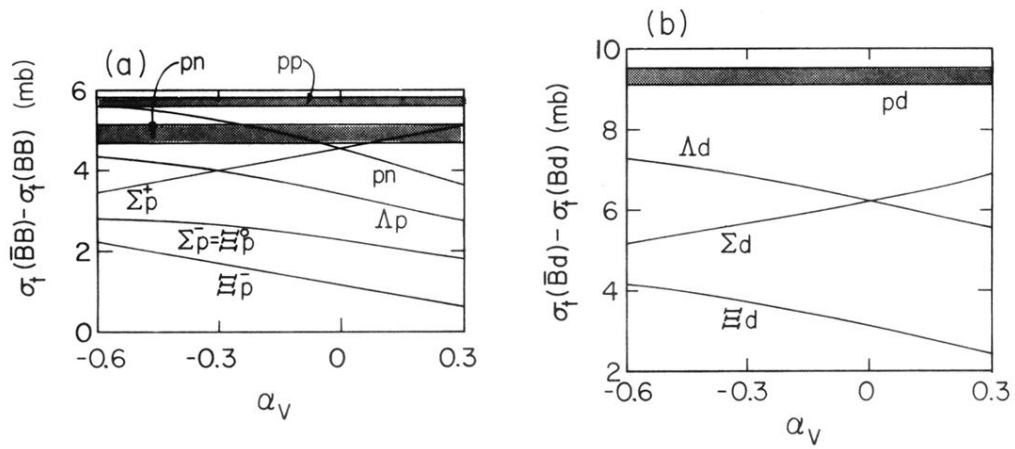[68]J. Lach, Fermilab workshop on short-lived beams, 1975 (unpublished).

FIG. 5. Baryon-antibaryon total-cross-section differences on (a) nucleon and (b) deuteron targets, as functions of the coupling parameter $\alpha_V = D/F$ for the vector-meson trajectories, at 50 GeV/$c$. The $\rho$ and $\omega^0$ trajectories are assumed to be exchange-degenerate for the nucleon-target predictions. Experimental data, shown as shaded bands, are from Carroll *et al.*, Ref. 9.